Available online at www.sciencedirect.com

SciVerse ScienceDirect

Ceramics International 39 (2013) 6813–6820

CERAMICS INTERNATIONAL

www.elsevier.com/locate/ceramint

Laser ablation behavior and mechanism of C/SiC composite

Yonggang Tong*, Shuxin Bai, Hong Zhang, Yicong Ye

College of Aerospace and Materials Engineering, National University of Defense Technology, Changsha 410073, PR China

Received 24 November 2012; received in revised form 10 January 2013; accepted 7 February 2013
Available online 13 February 2013

Abstract

A pulsed laser was used to investigate the ablation behavior and mechanism of C/SiC composite. The results indicated that linear ablation rate of the composite increased with increasing laser power densities and decreased with prolonged ablation time. Three ablation regions were identified on the ablated surface. The ablation center exhibited a needle-like structure with taper-ended carbon fibers standing on the ablation surface filled with some nano-structure carbon sheet. Many spheric SiC particles were deposited in the transitional zone. The ablation edge region was covered by a SiO_2 layer. Furthermore, the ablation mechanisms of different regions were proposed.

Keywords: B. Composite; B. Microstructure; D. SiC; D. Carbon; Ablation

1. Introduction

Ablation is an erosive phenomenon with a removal of material by a combination of thermo-mechanical, thermo-chemical, and thermo-physical factors from high temperature, pressure and velocity of combustion flame [1]. Materials with outstanding thermo-mechanical and thermo-chemical properties are required for future engine components, in particular combustion chambers and expansion nozzles which are subjected to high thermal loads [2]. SiC ceramic matrix composite reinforced by continuous carbon fibers (C/SiC) is one of the most promising candidate materials for high-temperature components due to its unique properties such as low density, low coefficient of thermal expansion, high specific strength/modulus and excellent resistance to ablation [3–5]. Ablation resistance is one of the most important properties in evaluating the usability of the C/SiC composite. Great efforts should be devoted to the investigation on the microstructure evolution during ablation and the ablation mechanism of the C/SiC composite before its practical application in the ablation environment. The main experimental methods for ablation process are oxyacetylene flame ablation, plasma arc ablation and kerosene-liquid oxygen flame ablation [6–9]. During the past years, numerous work has been made on the ablation-resistant properties of the C/SiC composite by these experimental methods and great achievements have been made [10–12]. Recently, the laser beam has been used to evaluate the ablation-resistant properties of materials [13–16], which provide us more knowledge about the usability of materials and developing protection against laser irradiation. However, no reports are available on the laser ablation behavior of the C/SiC composite so far. In present work, an impulse laser beam was used to evaluate the ablation resistance of the C/SiC composite and the laser ablation behavior and ablation mechanism of the composite were investigated.

2. Experimental

2.1. Materials

The C/SiC composite used in the experiment was fabricated using a polymer infiltration and pyrolysis (PIP) method by Key Laboratory of Advanced Ceramic Fibers and Composites (National University of Defense Technology, Changsha, China). Three-dimensional braided carbon fiber preform was used as the reinforcement. Fiber volume fraction in x, y and z directions of the preforms were

*Corresponding author. Tel.: +86 731 4576147; fax: +86 731 4574791.
E-mail address: tygiaarh419@163.com (Y. Tong).

0272-8842/$ - see front matter
http://dx.doi.org/10.1016/j.ceramint.2013.02.012

8:1:1. Polycarbosilane (PCS), the precursor of SiC matrix, was synthesized in the laboratory. Divinylbenzene (DVB) was used as solvent and cross-linking reagent for PCS. The carbon fiber preforms were firstly infiltrated with PCS/DVB solution in vacuum at room temperature and the preforms filled with PCS/DVB solution were then cured at about 150 °C. Finally, in an inert atmosphere, the cured preforms were pyrolyzed at 1200 °C to form the SiC matrix. In order to densify the composites, the other several infiltration-cure–pyrolysis cycles were repeated. The details of the polymer infiltration and pyrolysis method were described elsewhere [17].

2.2. Ablation tests

The ablation properties of the C/SiC composite were tested by a pulsed laser in the air. The laser ablation equipment is a Nd: YAG pulsed laser (wave length 1.064 μm) with the following parameters: frequency 20 Hz, pulse width 1 ms, laser spot diameter about 1.5 mm. The laser power densities of 150, 500, 1000 and 1500 W/cm^2 were selected to test the composite's ablation properties. During the ablation testing, the C/SiC composite was located in a test chamber and was then vertically irradiated by the pulsed laser. Three samples were examined in each ablation testing. The ablation depth of C/SiC composite was given by the thickness change before and after the ablation testing, which was measured by a microscope. The linear ablation rate of the C/SiC composite was calculated by the eroded depth at the ablation center dividing the ablation time.

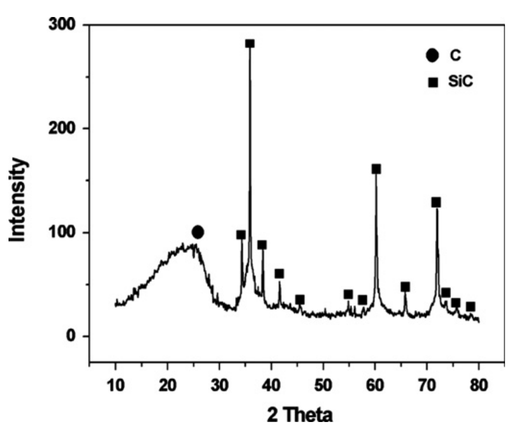

Fig. 1. XRD patterns of the C/SiC composite.

2.3. Characterization

The morphologies of the samples were observed by a Hitachi-S4800 scanning electron microscope (SEM). The chemical composition was examined by an energy dispersive spectroscopy (EDS). The phases were identified by X-ray diffraction (XRD, Rigaku D/Max 2550VB-) using a Ni-filtered Cu Kα radiation at a scanning rate of 5°/min and scanning from 10° to 80° of 2θ.

3. Results and discussion

3.1. Microstructure and composition of the C/SiC composite

Fig. 1 shows the XRD diffraction result of the C/SiC composite. It is indicated that the composite is composed of carbon and SiC phases. The cross-section micrographs of the C/SiC composite are shown in Fig. 2. As can be seen, the composite is generally dense with two kinds of pores. One is small distributing in the intra-fiber bundles and the other is larger locating in the inter-fiber bundles. The pores in the C/SiC composite can be attributed to the PIP process. The SiC matrix in the composite is derived from the pyrolysis of polycarbosilane. A lot of small molecule gases are formed during the pyrolysis of the polycarbosilane. Thus, the pores are inevitable in the C/SiC composite prepared by the PIP process even though several repeated cycles were used to densify the composite. Apart from these pores in the composite, both the regions in the intra-fiber bundles and in the inter-fiber bundles are completely filled by the pyrolytic SiC.

3.2. Laser ablation behavior and mechanism of the C/SiC composite

Fig. 3 shows the linear ablation rate of the C/SiC composite versus the laser power densities. It is indicated that the linear ablation rate of the composite increases with increasing laser power densities. During the ablation process, the laser energy is absorbed by the composite with an

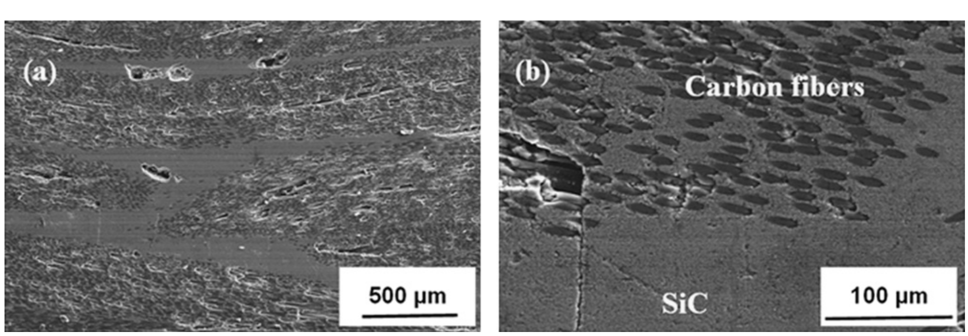

Fig. 2. Cross-section micrographs of the C/SiC composite (a) ×50 (b) ×350.

absorption coefficient, a heat conduction width and a heat penetration depth [18]. Along the heat penetration depth and conduction width, the conduction laser energy respectively decreases progressively from their input value, which in turn can affect the corresponding temperature distribution. The higher the laser power density is, the greater the heat penetration depth is. Therefore, the linear ablation rate increases with increasing the laser power densities.

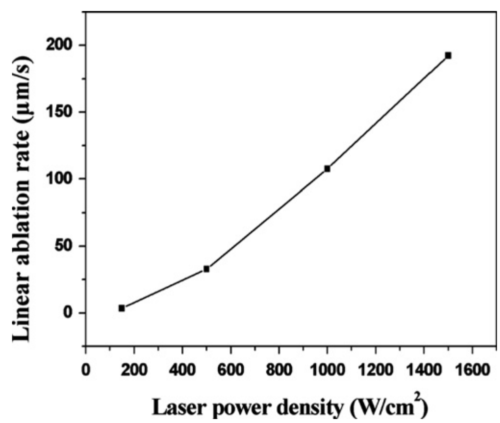

Fig. 3. Linear ablation rates of the C/SiC composite versus the laser power densities.

Fig. 4 shows the ablated surface morphologies of the C/SiC composite at 1000 W/cm^2 for 20 s. Three ablated regions can be distinguished on the ablated surface of the composite: region I ablation center with a deep pit, region II transitional zone with a lot of spheric particles and region III ablation edge covered by a white glassy layer (Fig. 4(a) and (b)). The detailed SEM observation of region I (Fig. 4(c) and (d)) shows that the ablation center exhibits a needle-like structure. Carbon fibers with taper ends stand on the ablation surface filled with some nano-structure sheet. EDS analysis (Fig. 5) was carried out to determine the composition of the nano-structure sheet and the three ablated regions. The results show that the nano-structure sheet is composed of carbon, which indicates that it is the nano carbon sheet. The spheric particles in the transitional zone are SiC phase with a composition of silicon and carbon owning the atom proportion of 54.47:45.53. The white layer in the region III ablation edge is SiO_2 composed of silicon and oxygen with the atom proportion of 33.58:66.42.

During the ablation testing, the center region was instantly heated to a very high temperature, which was

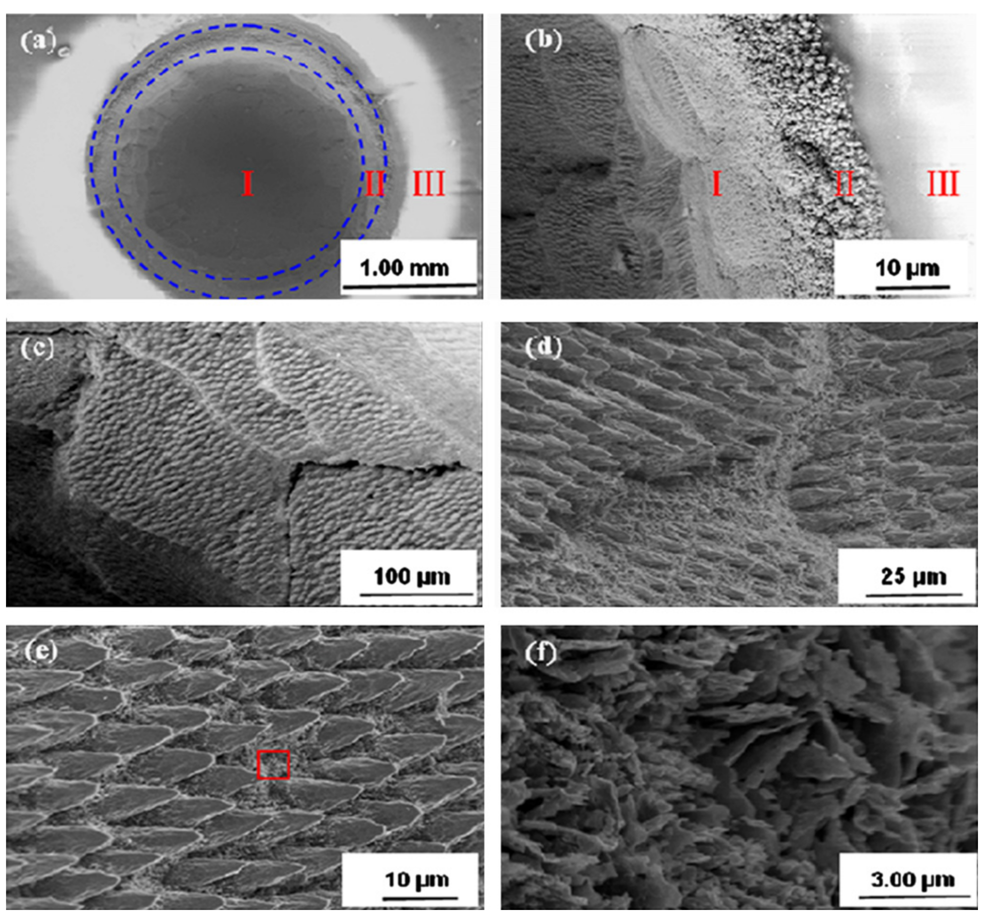

Fig. 4. The ablated surface morphologies of C/SiC composite at 1000 W/cm^2 for 20 s (a) and (b) three ablated regions on the ablated surface; (c) macro morphologies of the ablation center; (d) and (e) large magnification morphologies of the ablation center; (f) large magnification of the marked area in (e).

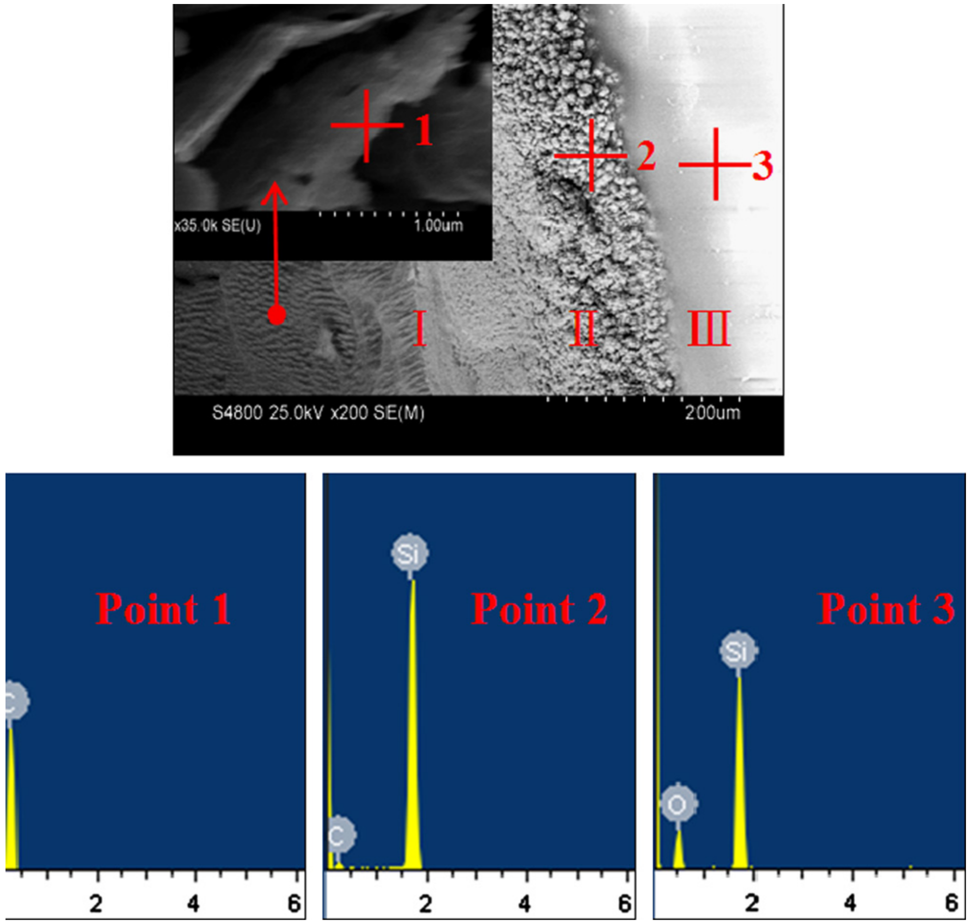

Fig. 5. EDS analysis of C/SiC composite surface after laser ablation at 1000 W/cm^2 for 20 s (point 1, nano carbon sheet; point 2, region II transitional zone; point 3, region III ablation edge).

estimated approximately higher than 3500 °C due to the large amount of ablated carbon fibers in the ablated center region. The SiC matrix reaches its decomposition and sublimation temperatures to form a hot mixture of gases and vapors due to its low thermally stable temperature [19]. The carbon fibers also get to its sublimation temperature to form a carbon vapor. The possible reactions in the ablation center region are as follows:

$$SiC\ (s) \rightarrow Si\ (g) + C\ (g) \tag{1}$$

$$SiC\ (s) \rightarrow SiC\ (g) \tag{2}$$

$$C\ (s) \rightarrow C\ (g) \tag{3}$$

$$SiC\ (s) + O_2\ (g) \rightarrow SiO_2\ (g) + CO\ (g) \tag{4}$$

$$SiC\ (s) + O_2\ (g) \rightarrow SiO\ (g) + CO\ (g) \tag{5}$$

$$C\ (s) + O_2\ (g) \rightarrow CO_2\ (g) \tag{6}$$

$$C\ (s) + O_2\ (g) \rightarrow CO\ (g) \tag{7}$$

The ablation testing was performed in the air and the carbon fibers and SiC matrix can be oxidized to form CO, CO_2, SiO and SiO_2 due to the reaction with oxygen according to Eq. (4–7) in the air. However, SiO, CO and CO_2 are gases and SiO_2 with the boiling point of 2230 °C [11] immediately gasified, which results in a positive pressure atmosphere on the ablation surface. The oxygen in the air on the ablation surface can be instantly exhausted and the oxygen in the outside air cannot diffuse into the atmosphere on the ablation surface due to the positive pressure kept by the gasses and vapors produced according to Eqs. (1–7). The oxidation of the carbon fibers and SiC just occurred at the very beginning and therefore, it was ignored, which would not affect the reasonability of our analysis. Exposed in the laser, the center area of the composite has the highest temperature [20] and it was severely ablated. The carbon fibers are thermally more stable than the SiC matrix and therefore, carbon fibers with taper ends protrude on the ablation surface without the SiC matrix (Fig. 4(c)).

In the ablated center region, the heat produced by the laser penetrates into the C/SiC composite along the direction of the laser beam. With the heat penetration depth increasing, the temperature at the region decreases. The ablation of carbon fibers is gradually alleviated and finally avoided along the heat penetration direction. Thus, the carbon fibers on the ablated surface show a needled-like structure with taper ends. Though the ablation of the carbon fibers is alleviative and avoidable along the heat penetration direction, the temperature is still high enough to result in the decomposition of SiC matrix and therefore, lots of grooves without SiC matrix are formed among the carbon fibers which are lower than the carbon fibers' taper ends. With the further depth increasing, the temperature in the grooves decreases. At a certain depth, the temperature becomes relatively low, at which the decomposition of SiC matrix is in a critical station. The decomposition of SiC according to Eq. (1) and sublimation of carbon fibers according to Eq. (3) during ablation lead to a carbon rich atmosphere on the ablation surface. In the grooves among carbon fibers, the SiC matrix decomposes while the temperature is not high enough for the sublimation of carbon fibers. Some nano carbon sheet deposits at the bottom of the grooves in the carbon rich atmosphere (Fig. 4(c, d)), which is deemed as the similar situation for the preparation of carbon nano tubes by laser ablation method [21,22]. The morphologies of the nano carbon sheet are more clearly seen in Fig. 6. The thickness of nano carbon sheet is less than 100 nm and most of its normal direction is vertical to the carbon fibers' axial direction.

At the transitional zone of the ablation surface, the conducted heat and the corresponding heat penetration depth are much lower than those at the ablation center. It is not high enough to induce the decomposition, vapourization and sublimation of the SiC matrix. The mixed gases of C, Si and SiC escaped from the ablation center are cooled down and SiC grains re-nucleate and grow to spherical particles (see Fig. 4(b)). Though the temperature at the transitional zone is lower than the ablation center, it is believed to be high enough to lead to the volatilization of SiO_2. Thus, no SiO_2 was found at the transitional zone. At region III ablation edge, the heat is only conducted form the ablation center and the temperature is the lowest. The C/SiC composite is just oxidized and SiO_2 resulted from the oxidation of SiC matrix cannot be volatilized. The as-irradiated region is covered by a white glassy SiO_2 layer (Fig. 4(a)). The electrical conductivity of SiO_2 is not very well. Thus, the layer shows a white fuzzy pattern under the scanning electron microscope. The three ablated regions can be more clearly seen on the surface morphologies of the C/SiC composite ablated at 1500 W/cm^2 (Fig. 7). Because of the higher laser power density, the composite was ablated more severely. More mixed gases escaped from the ablation center and therefore, more spherical SiC particles deposited on the transitional zone (Fig. 7(b)).

Fig. 8 shows the surface morphologies of the C/SiC composite ablated at 150 W/cm^2 for 20 s. As can be seen, only a little amount of carbon fibers in the center region was ablated. Most of carbon fibers remain their original shape, which can be contributed to the low temperature heated by the low laser power density. Nevertheless, the SiC matrix among the carbon fibers decomposed and the nano carbon sheet was formed (the same situation on the surface of the composite ablated at 1000 W/cm^2 and 1500 W/cm^2), which indicated that the temperature on the composite surface ablated at 150 W/cm^2 is high enough to induce the decomposition of SiC matrix. However, that temperature is not

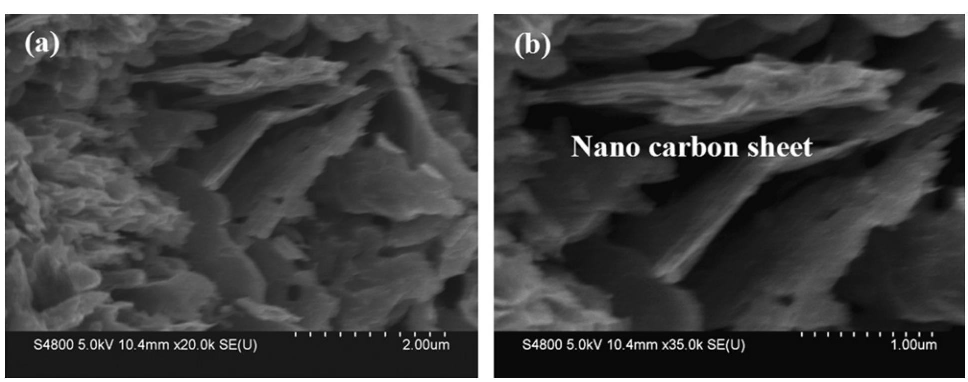

Fig. 6. Morphologies of the nano carbon sheet.

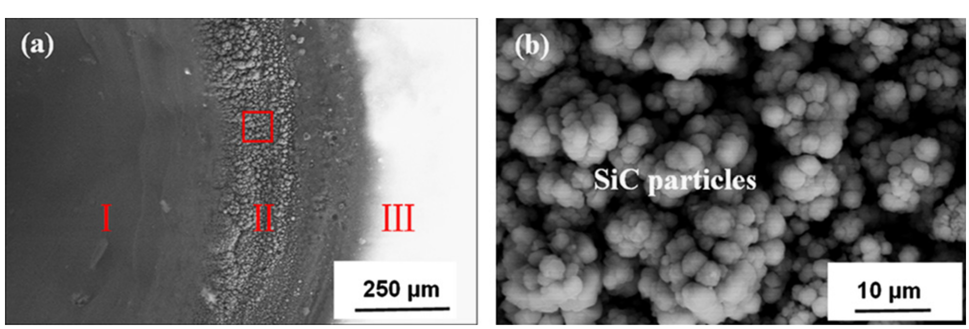

Fig. 7. Ablated surface morphologies of the C/SiC composite at 1500 W for 20 s (a) three ablated regions on the ablated surface; (b) SiC particles deposited at the transitional zone.

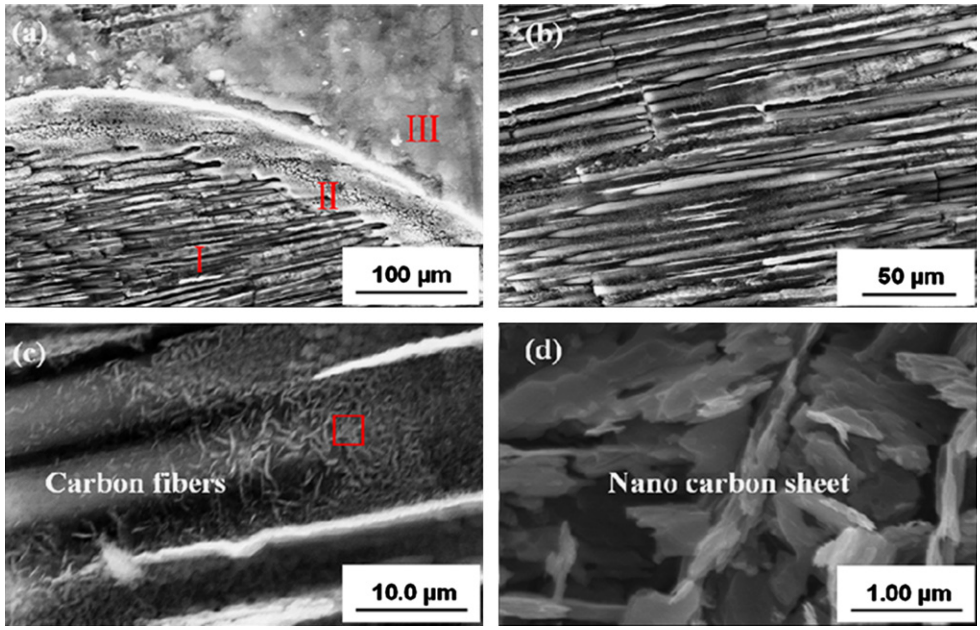

Fig. 8. Ablated surface morphologies of the C/SiC composite at 150 W/cm^2 for 20 s (a) three ablated regions on the ablated surface; (b) and (c) the ablation center; (d) large magnification of the marked area in (c).

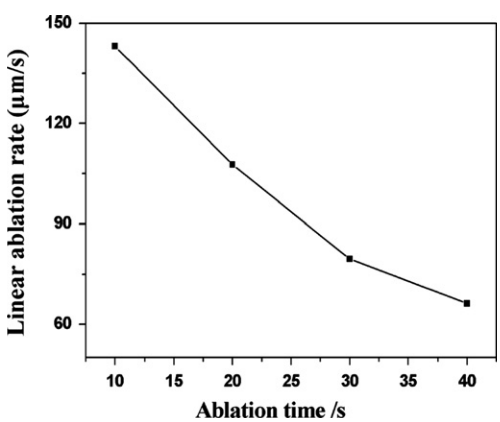

Fig. 9. Linear ablation rates of the C/SiC composite versus the ablation time at 1000 W/cm^2.

sufficient to lead to the sublimation of the carbon fibers. The ablated surface mainly shows the ablation of SiC matrix.

Fig. 9 shows the linear ablation rates of the C/SiC composite versus the ablation time at 1000 W/cm^2. It is indicated that the linear ablation rate of the C/SiC composite decreases with prolonged ablation time. The reasons can be concluded in two aspects. For the one hand, the ablation depth increases with the extension of ablation time, which enlarges the distance from the ablated surface to the laser focus. The temperature heated by the laser beam decreases with the distance increasing from the irradiated surface of sample to the laser focus [23]. Actually, the temperature on the ablated surface decreases with the delay of ablation time because of the deviation of the laser's focus [24]. For the other, a positive pressure mixed gas is formed during ablation process, which not only scatters the laser but also entrain a lot of heat on the ablation surface. The surface morphologies of the C/SiC composite ablated at 1000 W/cm^2 for different time show the same three ablated regions after the composite ablated at different laser power densities (not shown).

The laser ablation behavior of materials strongly depends on their structures and properties [25]. For the composites, the laser ablation mechanism can be very complicated, since their chemical and thermal properties are changed considerably under the laser irradiation. In order to understand the laser ablation processes of the C/SiC composite, an ablation model based on the previous characterization results and discussion was proposed (Fig. 10). As aforementioned, the temperature at the ablated center (region I) is the highest. The SiC matrix reaches its decomposition and sublimation temperatures to form a hot mixture of gasses and vapors and the carbon fiber gets to its sublimation temperature to form a carbon vapor, which results in a positive carbon rich atmosphere on the ablated surface. Nano carbon sheet is formed in the grooves among the protuberant carbon fibers where the temperature can lead to the decomposition of SiC matrix but is not high enough to result in simulation of carbon fibers. The laser ablation of the C/SiC composite is dominated by the decomposition and simulation process at the ablated center. With the proceeding of the laser ablation, the positive gases escape from the surface of the ablated center. Some of them deposit at the transitional zone (region II) where the temperature is relatively low and not high enough to result in the decomposition of SiC. SiC particles are formed at the transitional zone and the region is protuberant on the ablated surface. At the ablation edge (region III), the temperature is the lowest among the three ablated regions. The C/SiC composite is just oxidized and

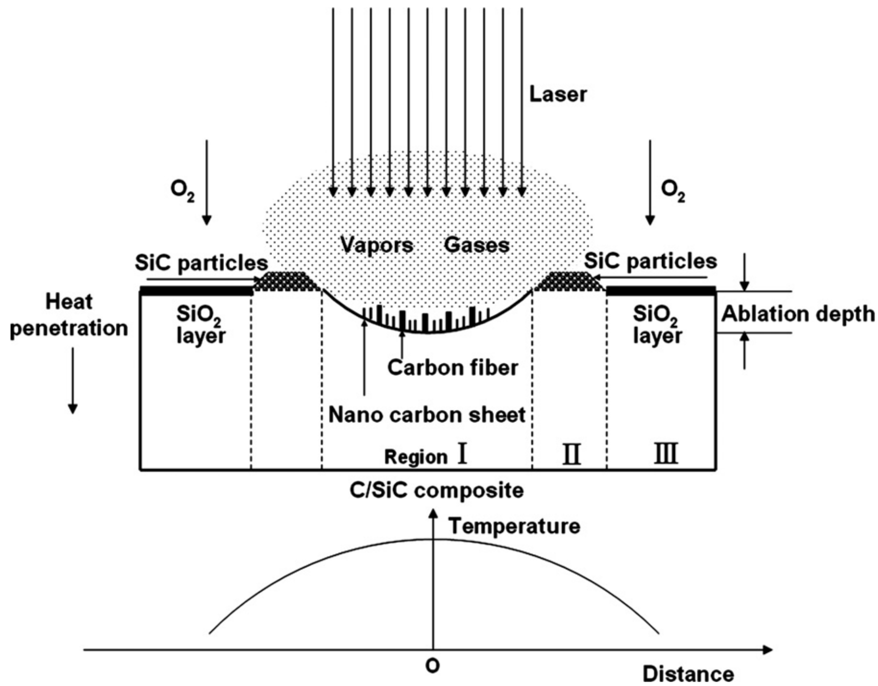

Fig. 10. Schematic of the laser ablation processes.

the region is covered by a white glassy SiO_2 layer. The oxidation products of the C/SiC composite contain CO, CO_2, SiO and SiO_2. CO, CO_2 and SiO are gaseous [26] and escape from the ablated surface. Nevertheless, SiO_2 formed during the oxidation is in the liquid state, which can flow on to the carbon fibers and protects the C/SiC composite from further oxidation. The laser ablation for this region is dominated by the oxidation process.

4. Conclusion

(1) The linear ablation rate of the C/SiC composite increased with increasing laser power densities and decreased with prolonged ablation time.
(2) The ablation center of the C/SiC composite exhibited a needle-like structure with the taper-ended carbon fibers standing on the ablation surface filled with some nano-structure carbon sheet. The laser ablation is dominated by the decomposition and simulation process at the ablated center.
(3) SiC particles were formed at the transitional zone and the region is protuberant on the ablated surface.
(4) The ablation edge region is covered by a white glassy SiO_2 layer and the laser ablation for this region is dominated by the oxidation process.

References

[1] D.L. Schmidt, Ablative polymers in aerospace technology, in: G.F. D'Alelio, J.A. Parker (Eds.), Ablative Plastics, Marcel Dekker, New York, 1971, pp. 1–39.
[2] S. Beyer, S. Schmidt, P. Peres, M. Bouchez, Advanced ceramic matrix composite materials for current and future propulsion system applications, AIAA, 2005 2005–3644.
[3] S. Beyer, H. Knabe, F. Strobel, Development and testing of C/SiC components for liquid rocket propulsion applications, AIAA, 1999 99–2896.
[4] S.K. Mital, P.L.N. Murthy, Characterizing the properties of a C/SiC composite using micromechanics analysis, AIAA, 2001 2001–1363.
[5] S.A. Chen, H.F. Hu, Y.D. Zhang, X.B. He, M. Mei, Rapid densification of C/SiC composites by joint processes of CLVD and PIP, Materials Letters 65 (2011) 3137–3139.
[6] B. Yan, Z.F. Chen, J.X. Zhu, J.Z. Zhang, Y. Jiang, Effects of ablation at different regions in three-dimensional orthogonal C/SiC composites ablated by oxyacetylene torch at 1800 °C, Journal of Materials Processing Technology 209 (2009) 3438-3443.
[7] D. Zhao, C.R. Zhang, H.F. Hu, Y.D. Zhang, Ablation behavior and mechanism of 3D C/ZrC composite in oxyacetylene torch environment, Composites Science and Technology 71 (11) (2008) 1392–1396.
[8] Z.Q. Li, H.J. Li, S.Y. Zhang, J. Wang, W. Li, F.J. Sun, Effect of reaction melt infiltration temperature on the ablation properties of 2D C/C–SiC–ZrC composites, Corrosion Science 58 (2012) 12–19.
[9] X.T. Shen, K.Z. Li, H.J. Li, Q.G. Fu, S.P. Li, F. Deng, The effect of zirconium carbide on ablation of carbon/carbon composites under an oxyacetylene flame, Corrosion Science 53 (2011) 105–112.
[10] Z.F. Chen, D. Fang, Y.L. Miao, B. Yan, Comparison of morphology and microstructure of ablation centre of C/SiC composites by oxyacetylene torch at 2900 and 3550 °C, Corrosion Science 50 (2008) 3378–3381.
[11] D. Fang, Z.F. Chen, Y.D. Song, Z.G. Sun, Morphology and microstructure of 2.5 dimension C/SiC composites ablated by oxyacetylene torch, Ceramics International 35 (2009) 1249–1253.
[12] S. Wu, L. Chen, L. Qian, J.B. Zhang, J.F. Pan, C.J. Zhou, et al., Ablation properties of C/C–SiC composites by precursor infiltration and pyrolysis process, Journal of the Chinese Ceramic Society 36 (7) (2008) 973–984.
[13] Q.M. Liu, L.T. Zhang, F.R. Jiang, J. Liu, L.F. Cheng, H. Li, et al., Laser ablation behaviors of SiC–ZrC coated carbon/carbon composites, Surface and Coatings Technology 205 (17–18) (2011) 4299–4303.
[14] G.D. Li, X. Xiong, K.L. Huang, Ablation mechanism of TaC coating fabricated by chemical vapor deposition on carbon-carbon composites, Transactions of Nonferrous Metals Society of China 19 (2009) 689–695.

[15] A. Slocombe, L. Li, Laser ablation machining of metalrpolymer composite materials, Applied Surface Science 154–155 (2000) 617–621.

[16] S. Costil, S. Lukat, C. Langlade, C. Coddet, Surface modification of ceramic matrix composites induced by laser treatment, Applied Surface Science 255 (2008) 2425–2432.

[17] K. Jian, Z.H. Chen, Q.S. Ma, H.F. Hu, W.W. Zheng, Effects of polycarbosilane infiltration processes on the microstructure and mechanical properties of 3D–Cf/SiC composites, Ceramics International 33 (2007) 905–909.

[18] J.F. Ready, Effects due to absorption of laser radiation, Journal of Applied Physics 36 (1965) 462–470.

[19] Y.S. Pan, Y.D. Xu, Z.F. Chen, L.F. Chen, L.T. Zhang, D.S. Xiong, Ablation properties analysis of 2D C/SiC composites, Ordnance Material Science and Engineering 29 (2006) 17–21.

[20] X.Y. Tan, D.M. Zhang, F. Mao, Z.H. Li, Yi Di, X.Z. Zhang, Theoretical and experimental study of energy transportation and accumulation in femtosecond laser ablation on metals, Transactions of Nonferrous Metals Society of China 19 (2009) 1645–1650.

[21] T. Guo, P. Nikolaev, A. Thess, Catalytic growth of single walled nanotubes by laser vapourization, Chemical Physics Letters 243 (1995) 49–54.

[22] M. Yudasaka, T. Komatsu, T. Ichihashi, S. Iijima, Single wall carbon nanotube formation by laser ablation using double-targets of carbon and metal, Chemical Physics Letters 278 (1997) 102–106.

[23] M. von Allmen, Laser-beam interactions with materials, Physical Principles and Applications, Springer-Verlag, Berlin, 1987.

[24] C.W. Sun, Q.S. Lu, Z.X. Fan, Laser irradiation effect, National Defense Industry Press, Beijing, 2002.

[25] B.N. Chichkov, C. Momma, S. Nolte, A. Alvensleben, A. Tünnermann, Femtosecond, picosecond and nanosecond laser ablation of solids, Applied Physics A 63 (1996) 109–115.

[26] R. Naslain, A. Guette, F. Rebillat, S. Legallet, F. Lamouroux, L. Filipuzzi, et al., Oxidation mechanisms and kinetics of SiC-matrix composites and their constituents, Journal of Materials Science 39 (2004) 7303–7316.